

A Measurement of the Contamination in [O III] $\lambda 5007$ Surveys of Intracluster Stars and the Surface Density of $z = 3.13$ Ly α Galaxies

Robin Ciardullo¹

*Department of Astronomy and Astrophysics, The Pennsylvania State University
525 Davey Lab, University Park, PA 16802*

`rbc@astro.psu.edu`

John J. Feldmeier¹

*Department of Astronomy, Case Western Reserve University 10900 Euclid Ave.
Cleveland, OH 44106-1712*

`johnf@eor.astr.cwru.edu`

Kara Krelove

*Department of Astronomy and Astrophysics, The Pennsylvania State University
525 Davey Lab, University Park, PA 16802*

`kara@astro.psu.edu`

George H. Jacoby

WIYN² Observatory, P.O. Box 26732, Tucson, AZ 85726

`jacoby@noao.edu`

and

Caryl Gronwall

*Department of Physics and Astronomy, The Johns Hopkins University
3400 N. Charles Street, Baltimore, MD 21218*

`caryl@pha.jhu.edu`

¹Visiting Astronomer, Cerro Tololo Inter-American Observatory, National Optical Astronomical Observatory, which is operated by the Association of Universities for Research in Astronomy, Inc., under cooperative agreement with the National Science Foundation.

²The WIYN Observatory is a joint facility of the University of Wisconsin-Madison, Indiana University, Yale University, and the National Optical Astronomy Observatory.

ABSTRACT

We present two pieces of evidence supporting the hypothesis that the bright [O III] $\lambda 5007$ sources found in Virgo’s intracluster space are intracluster planetary nebulae, rather than [O II] $\lambda 3727$ galaxies at $z \sim 0.35$ or Ly α sources at $z \sim 3.13$. First, we confirm the nature of five “overluminous” [O III] sources that are postulated to lie in front of M87: by examining the composite spectrum of these objects, we show that the weaker [O III] line at $\lambda 4959$ is definitely present at a strength $\sim 1/3$ that of [O III] $\lambda 5007$. The ratio demonstrates that, at most, only one of the five objects is a background galaxy. We then estimate the surface density of background emission-line objects by conducting a wide-field (0.13 deg^2) search at $\lambda 5019$ for faint emission line sources in a “blank field” located well away from any galaxy or cluster. We show that the density of blank field emission-line sources is significantly lower than the density of sources detected between the galaxies of Virgo, but in good agreement with the density of Ly α galaxies found by Hu, Cowie, & McMahon (1998). The implication is that background galaxies only account for $\sim 20\%$ of the planetary nebula candidates in Virgo’s intracluster fields.

Subject headings: galaxies: clusters: general — galaxies: interactions — planetary nebulae: general — cosmology: observations — galaxies: evolution — galaxies: formation

1. Introduction

A very powerful method for probing the history of galaxy clusters is through the observation and analysis of intracluster light (cf. Dressler 1984; Miller 1983; Merritt 1984; Moore, Quillis, & Bower 2000). Recently, this field has been revolutionized by on-band/off-band [O III] $\lambda 5007$ surveys for planetary nebulae (PNe) located between the galaxies of Fornax and Virgo. By searching for emission line objects on CCD frames and adopting reasonable values for the ratio of PNe to main sequence stars, Theuns & Warren (1997), Méndez et al. (1997), Ciardullo et al. (1998) and Feldmeier, Ciardullo, & Jacoby (1998) all concluded that a substantial fraction ($\gtrsim 20\%$) of the stellar mass of these clusters resides outside of any galaxy.

This result, however, is by no means secure. By comparing star counts in a Virgo intracluster field with counts performed on the *Hubble Deep Field*, Ferguson, Tanvir, & von Hippel (1998) concluded that only $\sim 11\%$ of Virgo’s stellar mass belongs to a diffuse

intergalactic component. In addition, the interpretation of Virgo’s [O III] $\lambda 5007$ sources as intergalactic planetary nebulae has been called into question by the *VLT/FORS* spectroscopy of Kudritzki et al. (2000). Although spectroscopic observations by Freeman et al. (2000) appear to confirm that most of the emission line sources identified by Ciardullo et al. (1998) and Feldmeier, Ciardullo, & Jacoby (1998) are, indeed, [O III] $\lambda 5007$ emitters in nearby intracluster space, the Virgo PN candidates observed by Kudritzki et al. are all background galaxies. If most of the emission-lines sources found in the [O III] surveys are also background galaxies, then many of the conclusions recently reached about intracluster starlight in Virgo and Fornax are incorrect, and the usefulness of planetary nebula surveys in intracluster space has to be reconsidered.

Here we report the results of two experiments designed to estimate the number of background galaxies expected in surveys of Virgo and Fornax intracluster planetary nebulae (IPNe). First, we describe spectroscopic observations of five planetary nebulae in the field of M87 that have been labeled by Ciardullo et al. (1998) as “overluminous” and therefore foreground to M87. We show that a composite spectrum made from these sources contains both [O III] $\lambda 5007$ and [O III] $\lambda 4959$ in the appropriate ratio. Consequently, it is likely that the majority of the overluminous objects in this field belong to the cluster. We then report the results of a 0.13 deg^2 on-band/off-band photometric survey at 5019 \AA of a “blank field” set well away from any nearby galaxy or cluster. We show that, although the density of “PN-like” sources in the field is not negligible, it is still five times smaller than the density derived for [O III] sources in Virgo. Thus, surveys for intracluster PNe remain a viable method for measuring the amount of stars stripped out of galaxies. Finally, we discuss the nature of the contaminating objects, and, using arguments based on emission line equivalent widths, conclude that most of these sources are emission-line galaxies at $z = 3.13$. Our results support the conclusions of Hu, Cowie, & McMahon (1998) that $\text{Ly}\alpha$ galaxies with monochromatic fluxes of $\lesssim 6 \times 10^{-17} \text{ ergs cm}^{-2} \text{ s}^{-1}$ and observed equivalent widths greater than 80 \AA are fairly common, although the density we derive is only one-half the Hu et al. value.

2. Spectroscopy of Candidate Intracluster Planetary Nebulae

In their on-band/off-band [O III] $\lambda 5007$ survey of planetary nebulae in the field of M87, Ciardullo et al. (1998) found that the planetary nebula luminosity function (PNLF) of the galaxy is distorted relative to the PNLFs of other galaxies. Specifically, in the outer part of the galaxy, M87’s PNLF does not have a sharp cutoff at its bright end; instead, the galaxy appears to contain a population of “overluminous” objects that are up to $\sim 0.6 \text{ mag}$ brighter

than the PNe seen in other galaxies. Because the number of these overluminous PNe scales with the survey area, and not galactic surface brightness, Ciardullo et al. concluded that these bright [O III] $\lambda 5007$ sources are not associated with M87. Instead, Ciardullo et al. hypothesized that the overluminous PNe belong to the Virgo Cluster as a whole, and are projected up to ~ 3 Mpc in front of M87.

To test this hypothesis, we used the *Hydra* multi-fiber spectrograph on the Kitt Peak WIYN telescope to obtain spectra of some of the overluminous PN candidates. Our specific spectrograph setup included *Hydra*’s 2-arcsec red sensitive fiber cables, the bench spectrograph’s 285 mm focal length camera, a SITe 2048×2048 CCD detector (4.3 e^- readnoise, gain of $1.7 \text{ e}^- \text{ ADU}^{-1}$), and an 860 lines mm^{-1} grating blazed at $30^\circ 9'$. When used in second order, this grating-camera-detector combination yielded spectra with a dispersion of $0.47 \text{ \AA pixel}^{-1}$ and a resolution of 0.77 \AA over the wavelength range between 4500 \AA to 5500 \AA . The total observation time for the setup was three hours; to facilitate the removal of cosmic rays, the observations were split into three one-hour exposures.

Nine objects with monochromatic [O III] $\lambda 5007$ fluxes greater than $1.0 \times 10^{-16} \text{ ergs cm}^{-2} \text{ s}^{-1}$ ($m_{5007} < 26.25$) were chosen for study. Since M87’s PNLF cutoff occurs at $m_{5007} = 26.35$ (Ciardullo et al. 1998; Jacoby, Ciardullo, & Ford 1990), these PN candidates are all significantly “overluminous” (by $\sim 2\sigma$) with respect to the galaxy, and can be interpreted as foreground intracluster stars. Unfortunately, due to a combination of factors, including astrometric and fiber-positioning errors, only five of the emission-line objects were detected.

The multifiber spectra were extracted, flatfielded, and wavelength calibrated using the IRAF package *dohydra*. A flatfield image taken at the beginning of the night served as the reference for tracing the spectra on the CCD frame; the wavelength calibration was performed using copper-argon comparison arcs taken before and after the exposure sequence. Sky subtraction was accomplished using the summed spectra of 49 sky fibers randomly placed around the galaxy. Since the sky in this wavelength region is faint and our observations were taken at moderately high ($R \sim 6000$) resolution, our results are independent of the accuracy of this subtraction.

The overluminous PN candidates are listed in Table 1, using the identification numbers of Ciardullo et al. (1998). Figure 1 displays the recorded spectra in the wavelength region between 4940 \AA and 5060 \AA . As the figure illustrates, the signal-to-noise of the spectra is extremely low; in all cases, we have only a bare detection of a single, unresolved emission line. The fact that the emission lines are unresolved does suggest that the objects are Virgo PNe, rather than background galaxies (or quasars), since the velocity widths of the latter objects would likely be greater than our $\sim 50 \text{ km s}^{-1}$ resolution. However, for any individual object, this possibility cannot be excluded.

Nevertheless, we can use the procedure of Freeman et al. (2000) to *statistically* show that the detected emission line is [O III] $\lambda 5007$. To do this, we start by assuming that the identification of [O III] $\lambda 5007$ is correct, and then shift each spectrum back into its rest frame. We then scale the data so that all the $\lambda 5007$ lines have equal weight, and co-add the spectra to create a single composite spectrum. This spectrum is displayed in Figure 2. As the figure illustrates, the increased signal-to-noise brings out an additional feature: [O III] $\lambda 4959$. If all five overluminous objects are indeed, intergalactic PNe, then this companion line should be $1/3$ the strength of $\lambda 5007$; if some of the objects are background galaxies, then the line ratio should be reduced by the fraction of contaminants.

The ratio of $\lambda 4959$ to $\lambda 5007$ in Figure 2 is 0.31 ± 0.03 , where the quoted error represents our estimate of the measurement uncertainty, and neglects factors associated with the changing efficiency of the spectrograph. Since this number is extremely close to $1/3$, it is likely that all of the overluminous $\lambda 5007$ sources are planetary nebulae: at most, only one of the five objects can be a contaminant. Moreover, since the sources are too bright to be PNe associated with M87, the best hypothesis remains that these objects belong to the Virgo Cluster as a whole, and are located on the near side of the cluster.

3. [O III] $\lambda 5007$ Imaging of a Blank Field

An alternative method of determining the importance of contamination in IPNe surveys is through the analysis of a control region. By measuring the surface density of point-like emission-line sources in the field, we can directly estimate the amount of contamination expected in cluster surveys. To perform this “blank field” experiment, we chose a high-latitude ($b = -49^\circ$) location in the southern hemisphere, $\alpha(2000) = 4^{\text{h}}01^{\text{m}}$, $\delta(2000) = -39^\circ42'$. This region of sky is located well away from any nearby cluster: it is 16° from the center of Fornax, and 2.4 from the nearest (small) galaxy in the Tully Catalog (Tully 1988). Aside from one faint radio source (PMN J0401–3944; Griffith & Wright 1993) and one $z = 0.26$ quasar (Osmer 14; Osmer 1982) no remarkable objects are known to be located within the $30' \times 30'$ field of our camera.

According to the H I and galaxy count data of Burstein & Heiles (1982), the foreground galactic reddening in the region is $E(B - V) = 0.0$; from the DIRBE/IRAS data of Schlegel, Finkbeiner, & Davis (1998), this number is $E(B - V) = 0.029$. For simplicity, in this paper we assume that the extinction is identically zero.

We observed the blank field on the nights of 1998 Nov 20, 21, 22, and 23 with the Big Throughput Camera (BTC) on the Cerro Tololo 4-m telescope. This mosaic CCD system

consists of a square array of four 2048×2048 Tektronix CCDs, each of which has a readnoise of $\sim 5 \text{ e}^-$, a gain of $2.4 \text{ e}^- \text{ ADU}^{-1}$ and a scale of $0''.43$ per pixel. The total area included on all four chips is 0.23 deg^2 , but due to the dithering procedure used to improve the flatfielding, the actual area surveyed was only 0.215 deg^2 . When we exclude the data of CCD #2, which has a slightly lower (but highly variable) quantum efficiency, and eliminate the areas around saturated stars and bad pixels, our effective survey region is further reduced to 0.13 deg^2 . Still, this is over six times larger than that of the deep, narrow-band $\text{Ly}\alpha$ surveys of Hu, Cowie, & McMahon (1998) and Steidel et al. (2000).

The on-band filter used for our experiment was the [O III] #2 Mosaic filter of Kitt Peak; this filter has a central wavelength of 5019 \AA and a full-width-at-half-maximum (FWHM) of 55 \AA at ambient temperature in the converging beam of the telescope. The off-band filter was Kitt Peak Mosaic filter [O III]+29, whose central wavelength and FWHM are 5305 \AA and 241 \AA , respectively. The total on-band exposure time for our four nights of observations was 285 minutes; this was split into four 1-hr exposures plus one 45-min exposure. Our off-band data consisted of 5 15-min exposures, for a total integration time of 75 min. All these data were taken under photometric conditions in $1''.1$ seeing.

The procedures used to reduce the data, identify emission-line objects, and measure their brightnesses, were identical to those used to search for intracluster planetary nebulae, and are fully described in Feldmeier (2000). After de-biasing and flatfielding the data, the on-band and off-band frames were co-added to create master images that were clipped of cosmic-rays. The frames were then searched for PN-like candidates in two different ways using the DAOPHOT and PHOT packages within IRAF. The first method involved performing photometry of all point sources on the frames, and constructing a color-magnitude diagram from the results. Objects with highly negative on-band minus off-band colors were flagged as PN-like sources (cf. Figure 3). In the second method, candidate sources were identified by searching for positive residuals on a “difference image” made by subtracting a scaled version of the off-band image from the on-band frame. These two techniques complement each other, in that each detects objects that the other method does not. Because the color-magnitude algorithm is susceptible to confusion by continuum sources near target objects (blends), the former analysis misses $\sim 5\%$ of the emission-line sources, even at bright magnitudes. Conversely, the subtraction technique detects virtually all the bright emission-line objects, but loses some of the fainter sources due to the larger noise of the difference frame. As we describe below, these two techniques, coupled with our chosen detection threshold for DAOFIND, optimized our ability to detect real emission-line sources, and kept the number of false detections at a manageable level.

After analyzing our on-band/off-band frames with both methods, a series of routines

were run to purge the candidate list of false detections. First, we removed objects which fell within the excluded regions around saturated stars and near bad pixels. We then ignored all objects for which the final detected signal-to-noise was less than four; such objects are almost always random noise fluctuations (cf. Ciardullo et al. 1987; Hui et al. 1993). Finally, we removed probable cosmic rays from our list by going back to the individual exposures which created the master on-band frames. Using apertures of the order of the seeing FWHM, we measured the magnitude of each candidate object on each individual frame. If, after correcting for sky transparency, one of the measurements was 5σ higher than the mean determined from the magnitudes on the other four frames, the object was deleted from the analysis.

Once the false detections and cosmic rays were eliminated, the remaining PN-like candidates were screened by eye to create the final list of $\lambda 5019$ sources. To be included in the list, an object had to be spatially unresolved on the on-band image, and completely invisible on the off-band frame. A total of nine such “PN-like” objects were found by our procedure.

To confirm the robustness of our algorithms, we tested our results in three different ways. First, we added artificial stars to the on-band (but not the off-band) image using the ADDSTAR task within DAOPHOT. We then ran our detection algorithms, and computed the fraction of objects recovered as a function of magnitude. Since our algorithms can work no better than that of the star-finding algorithm (DAOFIND; Stetson 1987), this analysis places a limit on the effectiveness of the search. The result of this simulation for one of the BTC CCDs is shown in Figure 4. As the figure illustrates, we are 90% complete down to an instrumental magnitude of $m_{inst} = 27.74$, and 50% complete to $m_{inst} = 28.19$. For consistency with other planetary nebula surveys, we adopt the 90% completeness limit, which is equivalent to a signal-to-noise of nine (Ciardullo et al. 1987; Hui et al. 1993), as this survey’s limiting magnitude.

As a second test, we ran our automated detection algorithms on frames of the Virgo Cluster that had been visually blinked as part of previous surveys for intracluster planetaries (Feldmeier, Ciardullo, & Jacoby 1998, 2001). Our new algorithms recovered all of the PN candidates above the DAOFIND completeness limit and 92% of all the previously known sources. Finally, two of us (J.J.F. and K.K.) independently blinked one of the BTC CCD fields by eye, and compared our results to those of the automated algorithm. In both cases, all objects brighter than $m_{inst} = 27.7$ that were found by eye were also recovered by the computer. We are therefore confident that our detection scheme is the best possible for finding faint emission-line sources in a blank field.

Once the objects were found, their equatorial positions were derived with respect to the reference stars of the USNO-A 2.0 astrometric catalog (Monet 1998; Monet et al. 1996). The

measured residual of our plate solution was $\sim 0''.2$, a number slightly less than the $0''.25$ external error associated with the catalog. On-band and off-band photometry was accomplished relative to bright field stars via the aperture photometry routines within IRAF. These data were then placed on the standard AB system by comparing large aperture measurements of field stars with similar measurements of the Stone (1977) and Stone & Baldwin (1983) spectrophotometric standards Feige 110, LTT 1020, LTT 3218, EG 21, and LTT 2415. The dispersion in the photometric zero point computed from these stars was 0.03 mag. Finally, we converted the on-band AB magnitudes to $\lambda 5007$ monochromatic fluxes using the techniques outlined in Jacoby, Quigley, & Africano (1987), under the assumption that the wavelength of the detected emission line lies near the bandpass center of the interference filter. For consistency with papers on extragalactic planetary nebulae, we define

$$m_{5007} = -2.5 \log F_{5007} - 13.74 \quad (1)$$

where F_{5007} represents monochromatic flux in $\text{ergs cm}^{-2} \text{ s}^{-1}$.

When placed on this standard system, the instrumental completeness limit of $m_{inst} = 27.7$ corresponds to an AB magnitude of $m_{AB}^{on} = 24.3$, or a $\lambda 5007$ magnitude of $m_{5007} = 27.0$. A similar analysis for the continuum frame reveals that the limiting AB magnitude of our off-band data is $m_{AB}^{off} = 24.7$. Coupled together, these two numbers imply that our $\lambda 5007$ survey should be complete to a monochromatic flux of $5.0 \times 10^{-17} \text{ ergs cm}^{-2} \text{ s}^{-1}$, which corresponds to an equivalent limit of $W_\lambda > 82 \text{ \AA}$ in the observer's frame.

4. The Density of Background Sources

Those objects which, had they been located in a cluster environment, would have been mistaken for intracluster planetary nebulae, are listed in Table 2. All the detected point-sources have *extremely large* equivalent widths: the smallest value is 212 \AA , and the median equivalent width is 273 \AA . These numbers are far above our detection threshold of 82 \AA , and demonstrate that the number of PN-like sources in the blank field is not sensitive to this quantity. The most important feature of the table, however, is its rather small number of objects. Only nine point sources brighter than our limiting magnitude of $m_{5007} = 27.0$ were detected in the 0.13 deg^2 region. This compares to nine objects brighter than $m_{5007} = 26.8$ in the lowest density Virgo field observed by Feldmeier, Ciardullo, & Jacoby (1998). Considering that the Feldmeier et al. field is less than half the area of this survey, the data imply that surveys for intracluster PNe are a viable way to probe the distribution of intracluster starlight.

The results, however, do suggest that some of the recent conclusions about intracluster

stars in Virgo and Fornax may be incorrect. For example, Feldmeier, Ciardullo, & Jacoby (1998) used the apparent luminosity of Virgo’s brightest [O III] $\lambda 5007$ sources and the planetary nebula luminosity function, to place an upper limit on the distance to the front edge of the system. Their distance of ~ 11.8 Mpc implied that Virgo is extremely elongated along the line-of-sight. Based on our blank field study, it is clear that field objects with large equivalent widths and line fluxes as large as $\sim 7 \times 10^{-17}$ ergs cm $^{-2}$ s $^{-1}$ do exist, and can be mistaken for intracluster planetaries. Thus, structural analyses that depend on one or two extremely bright objects may be incorrect. In the case of the M87 field, the spectroscopy of Section 2 demonstrates that the intracluster environment is indeed elongated: since the absolute magnitude of the [O III] $\lambda 5007$ PNLF bright-end cutoff is $M^* = -4.5$ (Ciardullo et al. 1989), the apparent magnitudes of Table 1 imply that the front side of Virgo is no more distant than 12.8 Mpc (i.e., ~ 1.6 Mpc in front of M87; Ciardullo et al. 1998). Unfortunately, without spectroscopy, similar limits cannot be placed on other regions of the cluster.

To quantify the fraction of contamination expected, Table 3 compares the density of intracluster [O III] sources detected in Fields 2-6 of Feldmeier, Ciardullo, & Jacoby (1998, 2001) to the results of this blank field experiment. The limiting magnitudes of the Feldmeier et al. fields are generally not as deep as the data presented here ($m \lesssim 26.8$), so the Virgo results have been extrapolated to a depth of $m_{5007} = 27.0$ using the standard form of the PNLF:

$$N(M) \propto e^{0.307M} [1 - e^{3(M^*-M)}] \quad (2)$$

Although the contamination rate fluctuates from field to field, Table 3 demonstrates that $\sim 20\%$ of the emission-line objects found by Feldmeier et al. are likely to be interlopers. Unfortunately, it is difficult to define this fraction more precisely. Due to the small number of objects detected in the blank field survey, the derived contamination rate is uncertain by at least 33%. Moreover, if the contaminating sources are, indeed, extragalactic background objects, some field-to-field fluctuation might be expected to arise from large-scale structure. Nevertheless, our photometrically derived contamination fraction is in good agreement with the value of 26% determined via spectroscopy of individual IPN candidates (Freeman et al. 2000).

A $\sim 20\%$ contamination rate, coupled with the distribution of magnitudes given in Table 2, explains why Kudritzki et al. (2000) found a large fraction of contaminants in their spectroscopic survey, but Freeman et al. (2000) did not. From the table, it is apparent that there are more faint emission-line sources in our blank sky field than bright sources. A maximum-likelihood analysis of the nine data points suggests that, in the magnitude range $m_{5007} < 27$, a power-law $\log N(m) = a + bm$, with slope $b \approx 1_{-0.3}^{+0.5}$ adequately represents the differential source counts. If this behavior continues to fainter magnitudes, then the apparent discrepancy between the results of Kudritzki et al. and Freeman et al. is simply a function

of which objects the authors chose to observe. Of the nine objects observed by Kudritzki et al., two are extremely bright, with [O III] $\lambda 5007$ magnitudes more than 0.7 mag brighter than the nominal PNLf cutoff. Since the PNLf’s decline at bright magnitudes is extremely rapid, blank field sources dominate at these magnitudes. Moreover, four of the Kudritzki et al. targets are extremely faint, with $m_{5007} > 27.5$. In this regime, the slope of the PNLf has reached its limiting value of 0.133. Since this number is ~ 7 times shallower than the background source count slope, a significant amount of contamination is again expected. Between these two extremes, however, the density of background objects is much less than the density of IPNe, and it is this range that Freeman et al. performed their observations.

If we adopt a slope of $b \sim 1$ for the luminosity function of the background objects, and normalize the counts so that the background contributes $\sim 20\%$ of the $m_{5007} < 27$ sources in Virgo’s intracluster space, then by $m_{5007} \sim 27.6$, the density of interlopers is more than half that of the intracluster stars. Of course, this result depends sensitively on the extrapolated slope of the background source counts. Nevertheless, because the faint-end slope of the PNLf is shallow, we can expect that at some point past $m_{5007} = 27$, the background sources will overwhelm the planetaries.

Our estimate of the contamination rate moves PN-based measurements of Virgo’s intracluster stars into better agreement with that determined from *HST* red giant star counts (Ferguson, Tanvir, & von Hippel 1998). However, because the vast majority of PN candidates brighter than $m_{5007} = 27.0$ are still likely to be genuine, a factor of ~ 2 discrepancy between the two estimates remains. One possible explanation for the difference may be small-scale structure in the distribution of the intracluster stars themselves. Observationally, there is evidence that the IPN are scattered non-uniformly in the Virgo cluster (Feldmeier 2000) and most theories for the creation of intracluster stars predict that the distribution of such objects should have filamentary structure (Moore et al. 1996). Since the *HST* field is much smaller (~ 5 sq. arcmin) than the IPN fields (~ 200 sq. arcmin), it is entirely possible that the difference between the IPN and *HST* estimates for Virgo’s intracluster star population reflect real fluctuations in the stellar background.

5. What are the Contaminating Sources?

To be detected via our on-band/off-band interference technique, an object must have an extremely strong emission line, with an observed equivalent width of $W_\lambda > 82 \text{ \AA}$. If the line is not [O III] $\lambda 5007$, then the two most plausible alternatives are [O II] $\lambda 3727$ at $z = 0.35$ (rest frame equivalent width $W_\lambda > 60 \text{ \AA}$) or $\text{Ly}\alpha$ at $z = 3.13$ ($W_\lambda > 20 \text{ \AA}$). The former option is possible, though unlikely. Most of our emission-line sources have

putative [O II] rest frame equivalent widths greater than 150 \AA ; the redshift surveys of Cowie et al. (1996), Hammer et al. (1997), and Hogg et al. (1998) have yet to find such extremely strong [O II] emitters (but see Stern et al. 2000). Moreover, if the emission-line sources are really [O II] galaxies at $z = 0.35$, then these objects must have absolute magnitudes between $-15.3 < M_B + 5 \log h < -15.0$. (The bright limit comes from the limiting magnitude of our off-band frame, while the faint limit is derived from our on-band flux limit of $5 \times 10^{-17} \text{ ergs cm}^{-2} \text{ s}^{-1}$ and the observed $\sim 150 \text{ \AA}$ upper limit for [O II] equivalent widths.) If we integrate the luminosity function for low-redshift [O II] emission-line galaxies (Ellis et al. 1996; Small, Sargent, & Hamilton 1997) between these two limits, and normalize to the volume of space surveyed by our 55 \AA FWHM filter ($\sim 800 h^{-3} \text{ Mpc}^3$ at $z = 0.35$), then we find that ~ 4 [O II] emission line galaxies should lie within our survey region. Since only $\sim 10\%$ of faint ($M_B > -19$) [O II] emission line galaxies have equivalent widths greater than our 60 \AA rest frame survey limit (Cowie et al. 1996; Hammer et al. 1997; Hogg et al. 1998), the implication is that $\lesssim 1$ of our strong emission-line sources is an [O II] galaxy.

On the other hand, it is likely that at least some of our emission-line sources are $\text{Ly}\alpha$ objects. In their spectroscopic follow-up of candidate intracluster planetary nebulae in Virgo, Kudritzki et al. (2000) found nine such objects. Similarly, in their deep narrow-band and spectroscopic searches of a 75 square arcmin region, Hu, Cowie, & McMahon (1998) found that $\text{Ly}\alpha$ sources with observed equivalent widths $W_\lambda > 90 \text{ \AA}$ are not rare. Specifically, these authors found that, down to a limiting flux of $\sim 1.5 \times 10^{-17} \text{ ergs cm}^{-2} \text{ s}^{-1}$, the density of $\text{Ly}\alpha$ emitters at $z \sim 3.4$ is $\sim 15,000 \text{ deg}^{-2}$ per unit redshift interval. Since only five out of the twelve emitters tabulated by Cowie & Hu (1998) have fluxes greater than our detection limit of $5 \times 10^{-17} \text{ ergs cm}^{-2} \text{ s}^{-1}$, their observations suggest that we should be able to detect ~ 38 such objects in our survey region.

In order to compare our results to the Cowie et al. numbers, we expanded our search criteria to include both resolved sources and sources detected in continuum. To do this, we followed the prescription of Herrero et al. (2001) and modified DAOFIND’s FWHM convolution kernel so that our program could detect non-stellar objects. We then re-ran our search algorithms on the BTC images, and flagged all objects (both stellar and non-stellar) with fluxes above the completeness limit and with equivalent widths greater than 82 \AA . (For objects with no continuum detection, we used the off-band frame’s 1σ upper limit in our calculation of equivalent width.) The 12 additional objects found in this search are listed in Table 4, and plotted as open circles in Figure 3. Figure 5 displays the on-band, off-band, and difference images of a sample of our strong line-emitters (both PN-like and otherwise), and finding charts for all the sources listed in Tables 2 and 4 are given in Figure 6. In total, we detected 21 strong emission-line sources in our 0.13 deg^2 survey region. Of the 12 additional sources, five are well-resolved with FWHM sizes in the range between $\sim 1''.1$ and

$\sim 2''.2$, and another three are marginally resolved. This size distribution (13 point sources, 3 marginally resolved objects, and 5 clearly resolved galaxies) appears roughly consistent with the distribution of half-light radii observed for Lyman-break galaxies (cf. Lowenthal et al. 1997). However, higher resolution images are needed to confirm this result.

Our surface density, coupled with the $\Delta z = 0.046$ bandpass of our filter, implies that the surface density of Ly α sources with monochromatic fluxes greater than 5×10^{-17} ergs cm $^{-2}$ s $^{-1}$ is ~ 3500 deg $^{-2}$ per unit redshift interval. This value is marginally lower (by 1.4σ) than the value derived by Hu, Cowie, & McMahon (1998). The discrepancy certainly is not serious, especially since both surveys may be affected by large-scale structure. By counting Lyman-break galaxies in $9' \times 9'$ regions, Adelberger et al. (1998) has estimated the cell-to-cell variance of $z \sim 3$ Lyman-break galaxies to be $\sigma^2 \sim 1.3 \pm 0.4$. However, the large-scale distribution of Ly α emitters may be quite different, and significant excursions from the mean are possible. For example, in their 5-m survey of a 78 square arcmin region of the sky, Steidel et al. (2000) detected ~ 25 $z = 3.09$ emission-line sources above our detection threshold. When scaled to the bandwidth of our $\lambda 5007$ filter, their data give a Ly α galaxy surface density of $\sim 17,000$ deg $^{-2}$ per unit redshift interval, a number almost five times larger than observed here. However, the Steidel et al. survey was directed at a large structure of galaxies, whose volume density is $\sim 6.0 \pm 1.2$ times higher than average. Thus, their result is consistent with our observations.

For an $H_0 = 65$ km s $^{-1}$ Mpc $^{-1}$, $q_0 = 0.5$ universe, our data imply that the space density of $z = 3.13$ galaxies with Ly α (EW) > 21 Å and $L(\text{Ly}\alpha) > 2.2 \times 10^{42}$ ergs s $^{-1}$ is 9.3×10^{-4} galaxies Mpc $^{-3}$. Note that these objects are undergoing a significant amount of star formation. If we neglect internal extinction and assume (as do Hu, Cowie, & McMahon 1998) that the Ly α to H α ratio of these objects is 8.7 (Brocklehurst 1971), then 10^{42} ergs s $^{-1}$ in Ly α corresponds to a star formation rate of $1 M_\odot$ yr $^{-1}$ (cf. Kennicutt 1983). This implies that all but one of the objects detected in this survey have star formation rates between 1 and $8 M_\odot$ yr $^{-1}$. This is consistent with the $z > 3$ star formation rates derived from the rest-frame UV flux measurements of Steidel et al. (1998).

Figure 7 plots the emission-line luminosity function of strong emission-line sources, under the assumption that the objects are, indeed, Ly α galaxies at $z = 3.13$. If we integrate the function over the range displayed in the figure, we obtain a measured star formation rate density of $\sim 0.003 M_\odot$ yr $^{-1}$ Mpc $^{-3}$. If we then extrapolate the luminosity function to the approximate limiting magnitude of Hu et al. using the assumption that the luminosity function flattens past $L \sim 2 \times 10^{42}$ ergs s $^{-1}$ in a manner similar to a Schechter (1976) function, then the total star formation rate density of emission line galaxies brighter than $\sim 7 \times 10^{41}$ ergs s $^{-1}$ is $\sim 0.004 M_\odot$ yr $^{-1}$ Mpc $^{-3}$. This value is roughly one-tenth that derived

from Lyman-break galaxies (Steidel et al. 1999).

Our value for the space density of Ly α emitters and their implied star formation rate density is a factor of ~ 2 smaller than that derived by Hu, Cowie, & McMahon (1998). Since the Hu et al. data are for a slice of the universe at $z = 3.4$, it is possible to interpret this decrease as being due to evolution. However, given the small difference in time between these two epochs (~ 0.2 Gyr) and the small number of galaxies detected, it is far too early for such a conclusion.

6. Conclusions

By studying a blank field located well away from any galaxy or cluster, we have found that surveys for intracluster planetary nebulae are not pristine. At monochromatic fluxes fainter than $\sim 6 \times 10^{-17}$ ergs $^{-2}$ s $^{-1}$ there is a non-negligible amount of contamination from field objects. The most likely source of this contamination is Ly α galaxies at $z \sim 3.13$; the data therefore suggest that the same techniques that allow 4-m telescopes to map out the distribution of intracluster PNe, can be used to determine the distribution of starbursting galaxies at high redshift.

Nevertheless, our observations confirm the presence of intracluster PNe in Virgo. The amount of background contamination is not nearly enough to explain the number of emission-line sources found in wide-field surveys of Virgo; based on our blank-field data, the contamination fraction is only $\sim 20\%$. This low number is confirmed by our spectroscopy of candidate intracluster PNe in the field of M87: the presence of [O III] $\lambda 4959$ in a composite spectrum of five “overluminous” objects implies that at least four of the objects are true planetary nebulae. Surveys for intracluster planetaries at magnitudes brighter than $m_{5007} \sim 27$ therefore remain an effective way of probing the dynamical history of nearby clusters.

We thank K. Freeman, R. Kudritzki, and R. Méndez for useful discussions about the results of their spectroscopy of intracluster PN candidates, and J.A. Tyson for his assistance with the BTC camera. This research made use of NED, the NASA Extragalactic Database, and was supported in part by NSF grants AST 92-57833 and AST-9529270.

REFERENCES

- Adelberger, K.L., Steidel, C.C., Giavalisco, M., Dickinson, M., Pettini, M., & Kellogg, M. 1998, *ApJ*, 505, 18
- Brocklehurst, M. 1971, *MNRAS*, 153, 471
- Burstein, D., & Heiles, C. 1982, *AJ*, 87, 1165
- Ciardullo, R., Jacoby, G.H., Feldmeier J.J., & Bartlett, R. 1998, *ApJ*, 492, 62
- Ciardullo, R., Ford, H.C., Neill, J.D., Jacoby, G.H., & Shafter, A.W. 1987, *ApJ*, 318, 520
- Ciardullo, R., Jacoby, G.H., Ford, H.C., & Neill, J.D. 1989, *ApJ*, 339, 53
- Cowie, L.L., & Hu, E.M. 1998, *AJ*, 115, 1319
- Cowie, L.L., Songaila, A., Hu, E.M., & Cohen, J.G. 1996, *AJ*, 112, 839
- Dressler, A. 1984, *ARA&A*, 22, 185
- Ellis, R.S., Colless, M., Broadhurst, T., Heyl, J., & Glazebrook, K. 1996, *MNRAS*, 280, 235
- Feldmeier, J.J. 2000, Ph.D. Thesis, Penn State University
- Feldmeier, J.J., Ciardullo, R., & Jacoby, G.H. 1998, *ApJ*, 503, 109
- Feldmeier, J.J., Ciardullo, R., & Jacoby, G.H. 2001, in preparation
- Ferguson, H., Tanvir, N.R., & von Hippel, T. 1998, *Nature*, 391, 461
- Freeman, K.C., Arnaboldi, M., Capaccioli, M., Ciardullo, R., Feldmeier, J., Ford, H., Gerhard, O., Kudritzki, R., Jacoby, G., Méndez, R.H., & Sharples, R. 2000, in *ASP Conf. Ser. #197, Dynamics of Galaxies: From the Early Universe to the Present*, ed. by F. Combes, G.A. Mamon, & V. Charmandaris (San Francisco, Astronomical Society of the Pacific), 389
- Griffith, M.R., & Wright, A.E. 1993, *AJ*, 105, 1666
- Hammer, F., Flores, H., Lilly, S.J., Crampton, D., Le Fèvre, O., Rola, C., Mallen-Ornelas, G., Schade, D., & Tresse, L. 1997, *ApJ*, 481, 49
- Herrero, J.L., Frattare, L.M., Salzer, J.J., Gronwall, C., & Kearns, K.E. 2001, submitted to *PASP*

- Hogg, D.W., Cohen, J.G., Blandford, R., & Pahre, M.A. 1998, *ApJ*, 504, 622
- Hu, E.M., Cowie, L.L., & McMahon, R.G. 1998, *ApJ*, 502, L99
- Hui, X., Ford, H., Ciardullo, R., & Jacoby, G. 1993, *ApJ*, 414, 463
- Jacoby, G.H., Ciardullo, R., & Ford, H.C. 1990, *ApJ*, 356, 332
- Jacoby, G.H., Quigley, R.J., & Africano, J.L. 1987, *PASP*, 99, 672
- Kennicutt, R.C., Jr. 1983, *ApJ*, 272, 54
- Kudritzki, R.-P., Méndez, R.H., Feldmeier, J.J., Ciardullo, R., Jacoby, G.H., Freeman, K.C., Arnaboldi, M., Capaccioli, M., Gerhard, O., & Ford, H.C. 2000, *ApJ*, 536, 19
- Lowenthal, J.D., Koo, D.C., Guzman, R., Gallego, J., Phillips, A.C., Faber, S.M., Vogt, N.P., Illingworth, G.D., & Gronwall, C. 1997, *ApJ*, 481, 673
- Méndez, R.H., Guerrero, M.A., Freeman, K.C., Arnaboldi, M., Kudritzki, R.P., Hopp, U., Capaccioli, M., & Ford, H. 1997, *ApJ*, 491, L23
- Merritt, D. 1984, *ApJ*, 276, 26
- Miller, G.E. 1983, *ApJ*, 268, 495
- Monet, D. 1998, *BAAS*, 30, 1427
- Monet, D., Bird, A., Canzian, B., Harris, H., Reid, N., Rhodes, A., Sell, S., Ables, H., Dahn, C., Guetter, H., Henden, A., Leggett, S., Levinson, H., Luginbuhl, C., Martini, J., Monet, A., Pier, J., Rieke, B., Stone, R., Vrba, F., & Walker, R. 1996, *USNO A - 1.0* a catalog of astrometric standards, U.S. Naval Observatory, Washington, D. C.
- Moore, B., Katz, N., Lake, G., Dressler, A., & Oemler, A. 1996, *Nature*, 379, 613
- Moore, B., Quillis, V., & Bower, R. 2000, in *ASP Conf. Ser. #197, Dynamics of Galaxies: From the Early Universe to the Present*, ed. by F. Combes, G.A. Mamon, & V. Charmandaris (San Francisco, Astronomical Society of the Pacific), 363
- Osmer, P.S. 1982, *ApJ*, 253, 28
- Schechter, P.L. 1976, *ApJ*, 203, 297
- Schlegel, D.J., Finkbeiner, D.P., & Davis, M. 1998, *ApJ*, 500, 525
- Small, T.A., Sargent, W.L.W., & Hamilton, D. 1997, *ApJ*, 487, 512

- Steidel, C.C., Adelberger, K., Dickinson, M., Giavalisco, M., Pettini, M., & Kellogg, M. 1998, *ApJ*, 492, 428
- Steidel, C.C., Adelberger, K.L., Giavalisco, M., Dickinson, M., & Pettini, M. 1999, *ApJ*, 519, 1
- Steidel, C.C., Adelberger, K.L., Shapley, A.E., Pettini, M., Dickinson, M., & Giavalisco, M. 2000, *ApJ*, 532, 170
- Stern, D., Bunker, A., Spinrad, H., & Dey, A. 2000, *ApJ*, 537, 73
- Stetson, P.B. 1987, *PASP*, 99, 191
- Stone, R.P.S. 1977, *ApJ*, 218, 767
- Stone, R.P.S., & Baldwin, J.A. 1983, *MNRAS*, 204, 347
- Theuns, T., & Warren, S.J. 1997, *MNRAS*, 284, L11
- Tully, R.B. 1988, *Nearby Galaxies Catalog*, (Cambridge: Cambridge University Press)

Fig. 1.— The spectra of five “overluminous” emission line sources in the field of M87; the ID numbers come from Ciardullo et al. (1998). Although the spectra have very low signal-to-noise, a single unresolved emission line, which is presumed to be [O III] $\lambda 5007$ is clearly visible. The fact that the emission line is unresolved at $\sim 50 \text{ km s}^{-1}$ resolution suggests that the line is not [O II] $\lambda 3727$ or $\text{Ly}\alpha$ emission from a background galaxy.

Fig. 2.— A composite spectrum of the five “overluminous” emission line sources, made using the assumption that the observed emission line is, indeed, [O III] $\lambda 5007$. In the spectrum [O III] $\lambda 4959$ is clearly visible, with a strength that is approximately 1/3 that of [O III] $\lambda 5007$. The second line confirms that the objects are local to the Virgo Cluster, and not background galaxies.

Fig. 3.— Excess emission in the narrow-band $\lambda 5019$ filter over the continuum for objects in our BTC field. The abscissa gives the monochromatic m_{5007} magnitude, while the ordinate shows the difference between the sources’ on-band and off-band AB magnitudes. Our on-band completeness limit of $m_{5007} = 27.0$ is represented by a vertical line; our equivalent width limit of 82 \AA is shown via the horizontal line. The dotted line represents an observer’s frame equivalent width of 300 \AA , and is shown for reference. The curve illustrates the expected 1σ errors in the photometry. The emission line sources discussed in the text are displayed as filled circles (for point-like objects) and open circles (for sources resolved in $1''.1$ seeing).

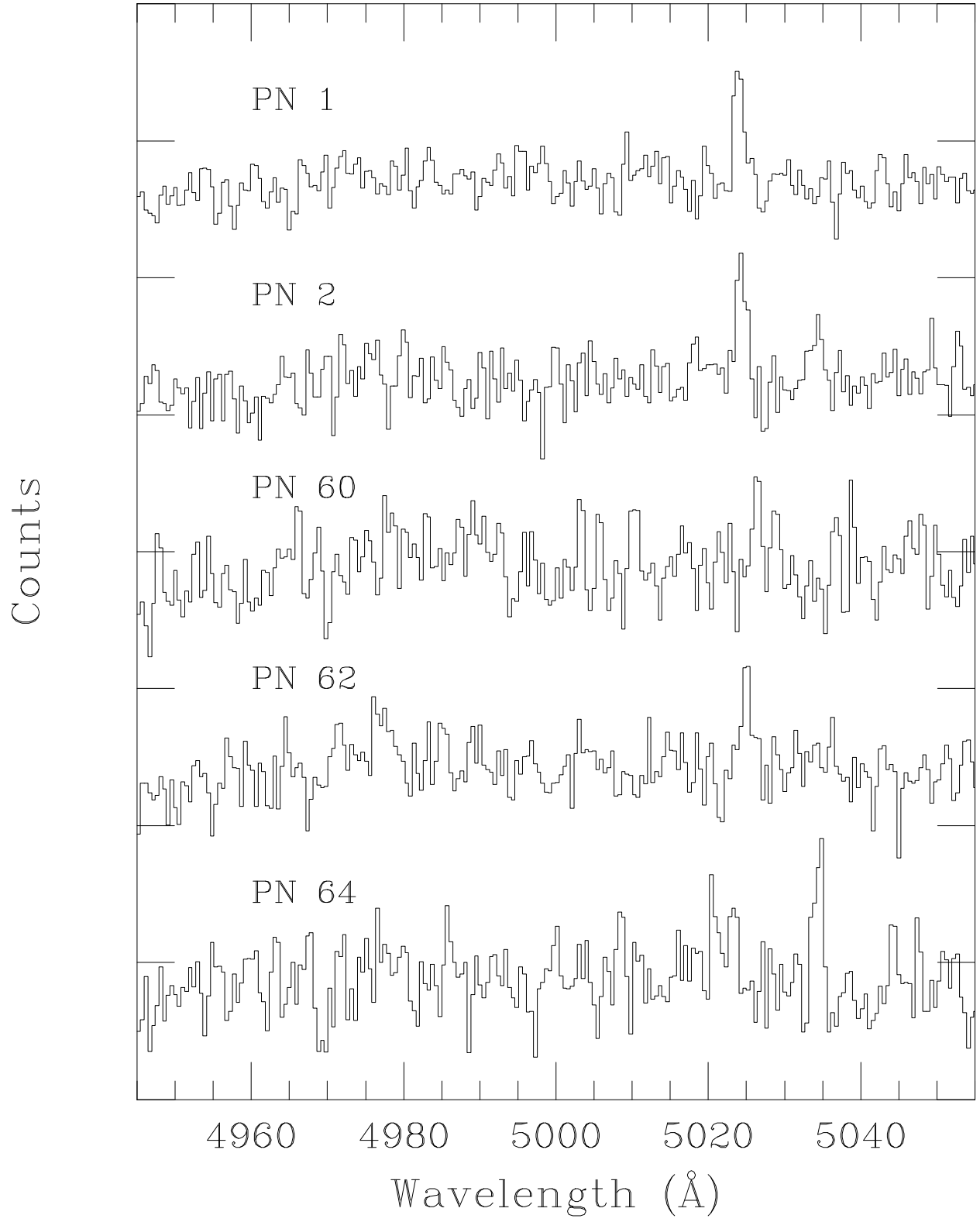
Fig. 4.— The fraction of artificial stars recovered on our on-band CCD frames as a function of instrumental magnitude. The open circles represent the efficiency of the DAOFIND detection algorithm, the solid squares plot the fraction of recoveries from the color-magnitude method, and the open triangles show the efficiency of detections on the difference image. The curves are spline fits through the data and are for illustration only. The solid vertical line denotes the 90% completeness limit of $m_{inst} = 27.44$, while the dashed line shows the 50% completeness limit at $m_{inst} = 28.19$. The simulations show that the color-magnitude method is the most efficient way of detecting faint emission line sources, but it fails to recover $\sim 5\%$ of objects at the bright end. Conversely, the difference method detects all of the brighter objects, but is not as effective at finding the faintest sources.

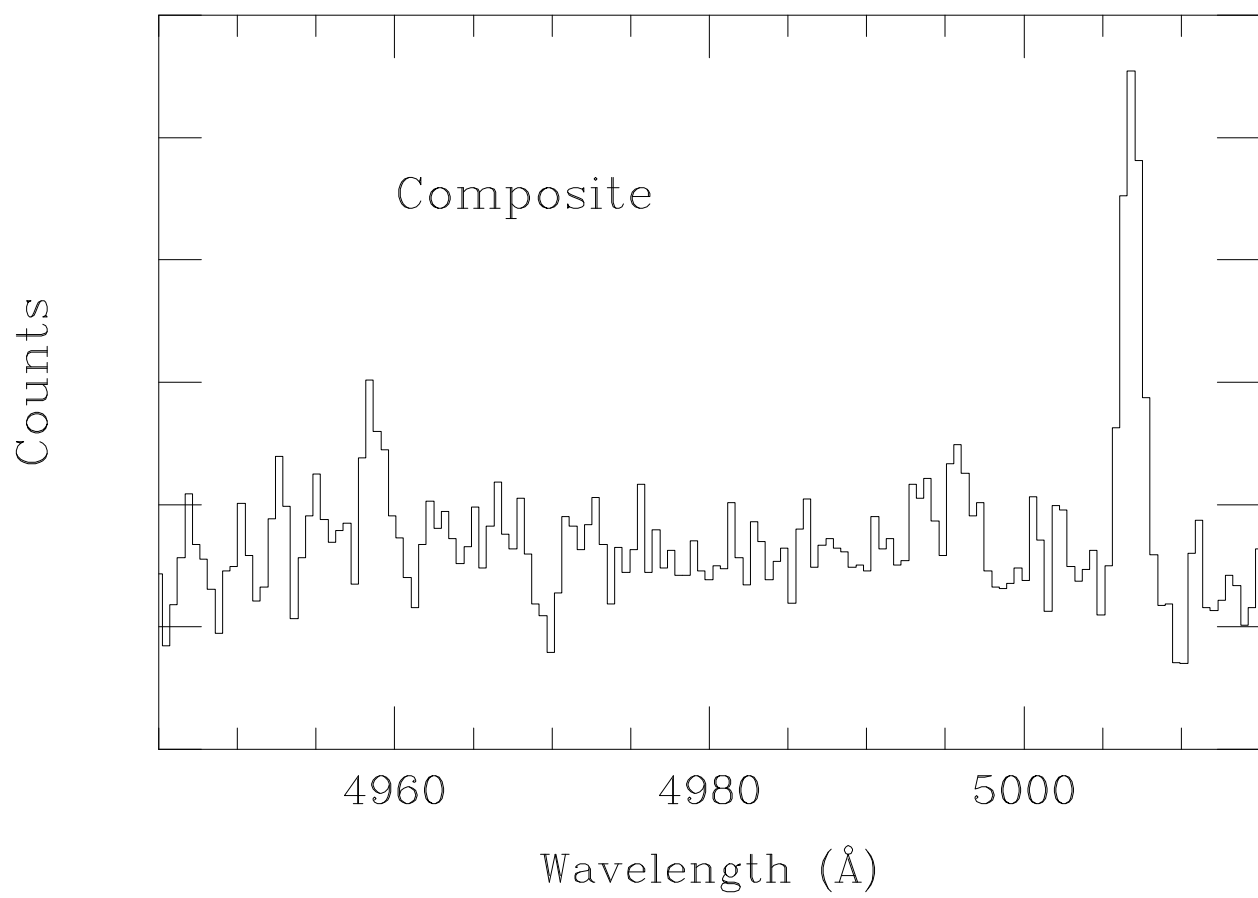
Fig. 5.— On-band, off-band, and difference images for objects 18 (top), 1 (middle) and 15 (bottom). Each frame is $30''$ on a side. North is up and east is to the left.

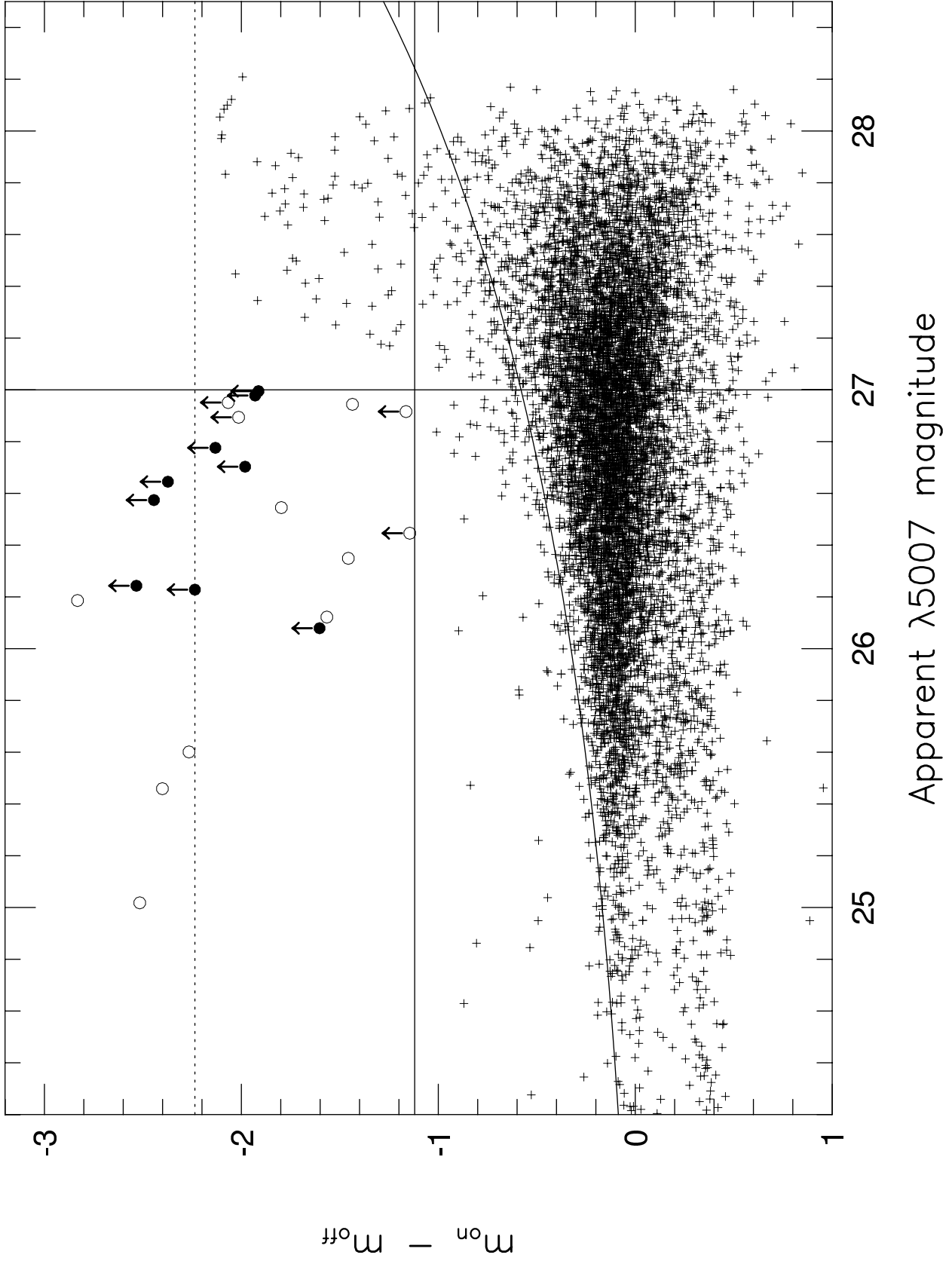
Fig. 6.— Finding charts for the strong emission-line sources found in this survey. Each frame is $1'$ on a side. North is up and east is to the left.

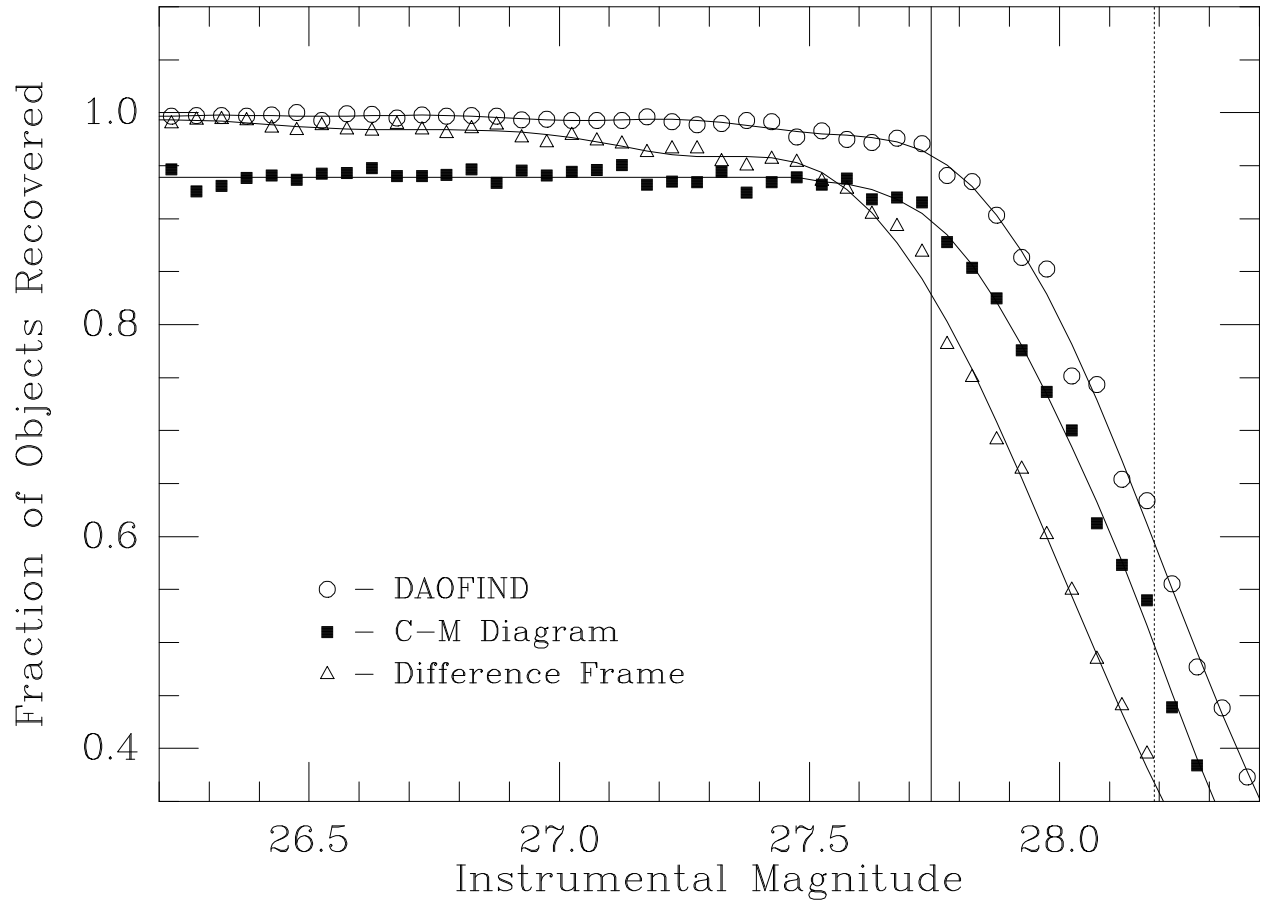
Fig. 7.— The luminosity function of all emission-line sources with equivalent widths greater than 82 \AA in the observer’s frame (or greater than 20 \AA in the rest frame of $\text{Ly}\alpha$). The

error bars in the y -direction represent the uncertainty due to counting statistics; the errors in the x -direction reflect the bin size (0.025 in log luminosity). For consistency with Cowie & Hu (1998), the data assume an $H_0 = 65 \text{ km s}^{-1} \text{ Mpc}^{-1}$, $q_0 = 0.5$, $\Lambda = 0$ cosmology. If we use the assumption that $10^{42} \text{ ergs s}^{-1}$ of $\text{Ly}\alpha$ photons is produced by $1M_\odot \text{ yr}^{-1}$ of star formation, then the integrated star formation rate density implied by the diagram is $\sim 0.004M_\odot \text{ yr}^{-1} \text{ Mpc}^{-3}$.









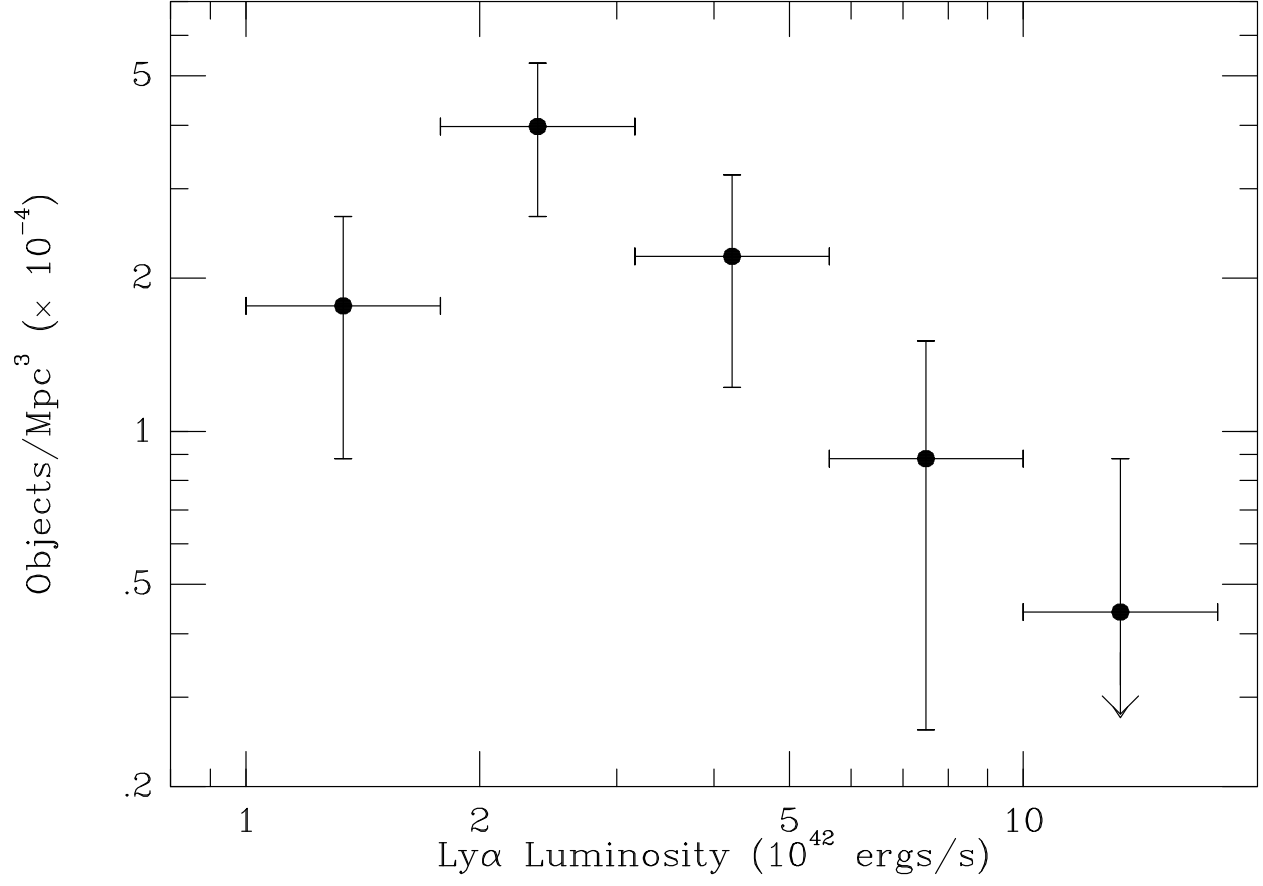


Table 1. Velocities of M87 Overluminous PN

| ID | $\alpha(2000)$ | $\delta(2000)$ | m_{5007} | V (km s ⁻¹) |
|----|----------------|----------------|------------|---------------------------|
| 1 | 12 30 49.38 | 12 20 58.4 | 25.63 | 1023 |
| 2 | 12 30 52.44 | 12 21 13.5 | 26.11 | 1041 |
| 60 | 12 30 38.95 | 12 28 13.8 | 26.01 | 1167 |
| 62 | 12 30 47.36 | 12 18 40.6 | 26.12 | 1084 |
| 64 | 12 30 42.14 | 12 29 13.9 | 26.21 | 1646 |

Table 2. Blank Field “PN-like” Emission-Line Objects

| ID | $\alpha(2000)$ | $\delta(2000)$ | m_{5007} | $\lambda 5007$ Flux (10^{-17} ergs cm ⁻² s ⁻¹) | Observed EW (Å) |
|----|----------------|----------------|------------|---|--------------------|
| 1 | 4 01 33.78 | −39 36 03.7 | 26.23 | 10.3 | $> 300 \pm 81$ |
| 2 | 4 01 19.63 | −39 40 04.6 | 26.70 | 6.7 | $> 228 \pm 66$ |
| 3 | 4 01 33.17 | −39 40 10.5 | 26.78 | 6.2 | $> 268 \pm 83$ |
| 4 | 4 00 31.83 | −39 49 01.4 | 26.98 | 5.2 | $> 216 \pm 70$ |
| 5 | 4 00 51.52 | −39 44 24.0 | 26.99 | 5.1 | $> 212 \pm 69$ |
| 6 | 4 02 54.95 | −40 01 35.2 | 26.08 | 11.8 | $> 273 \pm 69$ |
| 7 | 4 03 08.25 | −39 56 43.1 | 26.24 | 10.2 | $> 314 \pm 83$ |
| 8 | 4 00 26.29 | −39 56 10.2 | 26.57 | 7.5 | $> 373 \pm 107$ |
| 9 | 4 00 44.11 | −40 08 12.3 | 26.65 | 7.0 | $> 346 \pm 100$ |

Table 3. Estimates of Virgo Intracluster PN Contamination

| Field | Area of Field (arcmin ²) | Limiting Magnitude | Expected # of Contaminants | Extrapolated # of IPN Candidates | Contamination Rate |
|---------|---|-----------------------|-------------------------------|-------------------------------------|-----------------------|
| 2 | 252 | 26.8 | 4.8 | 18 | 26.7% |
| 3 | 241 | 27.0 | 4.6 | 21 | 21.9% |
| 4 | 158 | 26.6 | 3.0 | 21 | 14.3% |
| 5 | 200 | 26.1 | 3.8 | 30 | 12.7% |
| 6 | 204 | 26.8 | 3.9 | 14 | 27.3% |
| Average | | | | | $20.6 \pm 6.9\%$ |

Table 4. Other Blank Field Emission-Line Sources

| ID | $\alpha(2000)$ | $\delta(2000)$ | m_{5007} | m_{AB}^{off} | $\lambda 5007$ Flux (10^{-17} ergs cm ⁻² s ⁻¹) | Observed EW (Å) |
|----|----------------|----------------|------------|-----------------------|---|--------------------|
| 10 | 4 01 32.46 | −39 36 21.2 | 25.60 | 24.68 | 18.4 | 310 ± 51 |
| 11 | 4 01 27.66 | −39 44 06.6 | 26.45 | ... | 8.4 | $> 82 \pm 15$ |
| 12 | 4 01 30.45 | −39 37 05.3 | 26.89 | ... | 5.6 | $> 236 \pm 76$ |
| 13 | 4 01 29.55 | −39 42 50.1 | 26.94 | 25.19 | 5.3 | 122 ± 37 |
| 14 | 4 02 40.71 | −40 07 56.0 | 25.46 | 24.67 | 20.9 | 354 ± 53 |
| 15 | 4 02 34.61 | −40 03 43.7 | 26.35 | 24.62 | 9.2 | 115 ± 21 |
| 16 | 4 02 24.04 | −40 07 35.7 | 26.54 | 25.15 | 7.7 | 149 ± 34 |
| 17 | 4 03 04.49 | −40 01 48.2 | 26.92 | ... | 5.4 | $> 101 \pm 30$ |
| 18 | 4 01 31.68 | −40 07 45.0 | 25.02 | 24.34 | 31.3 | 401 ± 37 |
| 19 | 4 01 21.03 | −40 07 15.8 | 26.12 | 24.50 | 11.4 | 143 ± 18 |
| 20 | 4 00 31.02 | −39 55 43.8 | 26.19 | 25.83 | 10.7 | 551 ± 150 |
| 21 | 4 00 37.25 | −40 02 28.5 | 26.95 | ... | 5.3 | $> 122 \pm 33$ |

This figure "f5.jpg" is available in "jpg" format from:

<http://arxiv.org/ps/astro-ph/0110456v1>

This figure "f6a.jpg" is available in "jpg" format from:

<http://arxiv.org/ps/astro-ph/0110456v1>

This figure "f6b.jpg" is available in "jpg" format from:

<http://arxiv.org/ps/astro-ph/0110456v1>